Referee #2

** General comments **

The paper titled "Understanding the Long-term Trend of Organic Aerosol and the Influences from Anthropogenic Emission and Regional Climate Change in China" uses the CAM6-Chem model to analyze trends in organic aerosol (OA) in China from 1990 to 2019, identifying the roles of anthropogenic emissions and climate factors. The findings highlight a modest OA increase due to a rise in secondary organic aerosols (SOA) and a decrease in primary organic aerosols (POA), influenced by emission changes and warming. This work enhances our understanding of how emission controls and climate change have shaped OA dynamics over the past three decades. Generally, the paper is well-organized and demonstrates significant effort. However, the following questions need to be addressed prior to publication:

1. As the paper spans 30 years, significant changes in land use (due to deforestation, increased green space in urban areas, etc.) could have occurred. Does the work consider the effect of land use change? If not, it would be helpful to add a few lines discussing the impact of land use on biogenic emissions and resulting SOA concentrations.

Response: Thanks for your suggestion. Our study considered the impact of land use and land cover change (LUCC). The model captured the influence of LUCC through changes in the Leaf Area Index (LAI), which served as a key input parameter to represent the dynamic variations in LUCC (Nemani et al., 1996). BVOC emissions were further simulated online with the MEGAN model (Emmerson et al., 2018; Emmons et al., 2020; Guenther et al., 2012; Wang et al., 2022) incorporated within the CAM6-Chem. LUCC affected vegetation density, which in turn has significant impacts on plant transpiration, carbon absorption capacity and BVOC emissions (Fu and Liao, 2014). In the model, changes in LAI represent the impact of LUCC (such as deforestation, afforestation and urban greening expansion) on BVOC emissions. The simulation results (Fig. 3(f)) showed an increasing trend in BVOC emissions over the study period. This increase may partly attributed to a series of ecological restoration and conservation policies (Guo et al., 2022), such as the Grain-for-Green Program and Urban Ecological Civilization Construction (Yin et al., 2018). These policies effectively promoted the restoration

and expansion of vegetation while driving the continuous increase in urban greening areas. In addition, the warming trend (see Fig. 8(a)) may also enhanced the biosynthesis and emission of BVOC. These changes together contributed to the upward trend in SOA concentrations. We have added additional explanations between lines 380 and 390.

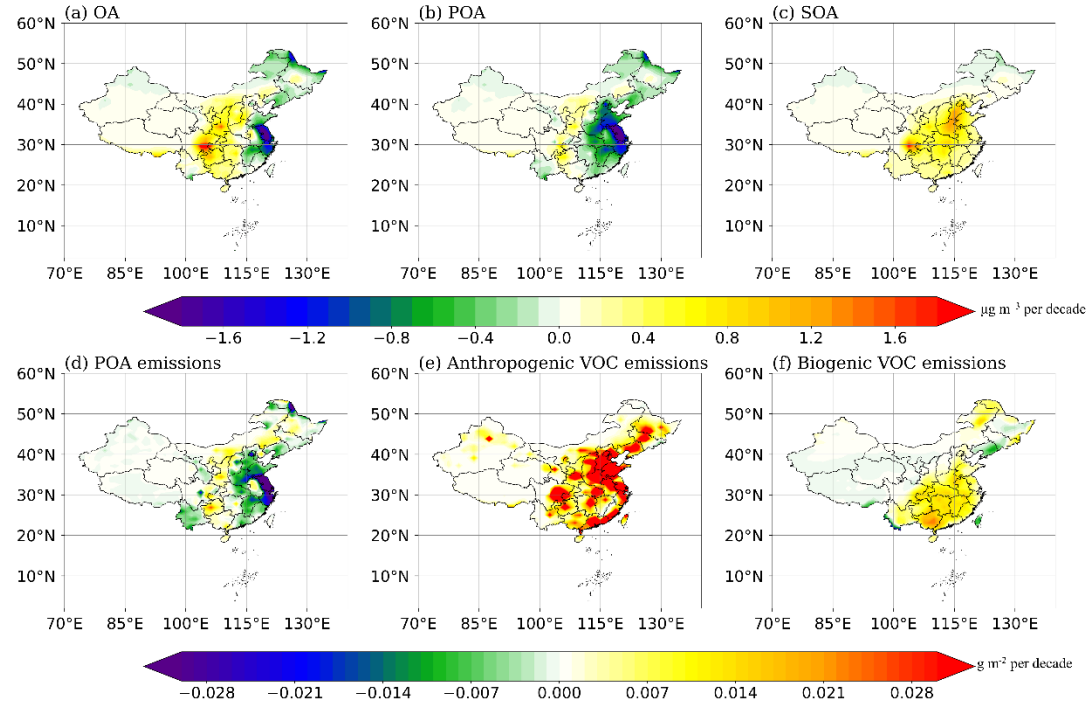

Figure 3: 1990 to 2019 annual average long-term trend of surface organic aerosols (OA; a; unit: μg m^{-3} per decade), primary organic aerosols (POA; b; unit: μg m^{-3} per decade), secondary organic aerosols (SOA; c; unit: μg m^{-3} per decade), primary organic aerosols emissions (d; unit: g m^{-2} per decade), anthropogenic volatile organic compounds emissions (e; unit: g m^{-2} per decade), biogenic volatile organic compounds emissions (f; unit: g m^{-2} per decade).

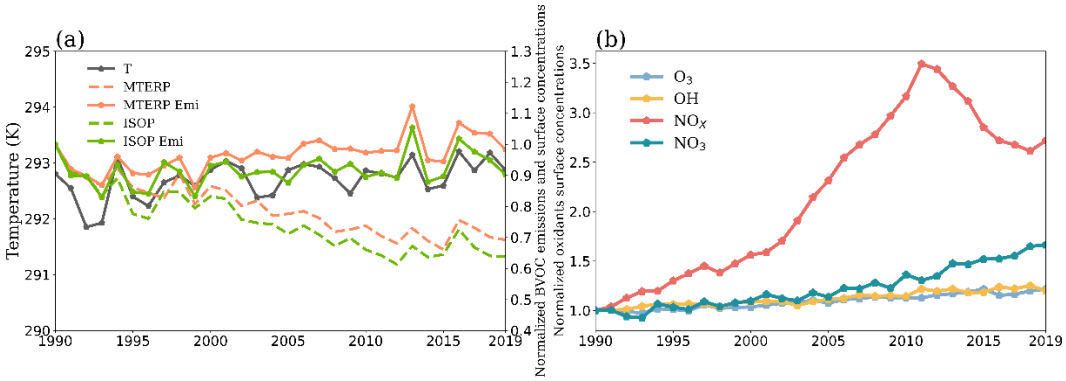

Figure 8: (a) 1990 to 2019 JJA time series of surface temperature (dark gray solid line; left Y axis; unit: K), relative changing ratio of surface concentrations for monoterpenes (orange dashed line; right Y axis; MTERP), isoprene (green dashed line; right Y axis; ISOP), monoterpenes emissions (orange solid line; right Y axis; MTERP Emi) and isoprene emissions (green solid line; right Y axis; ISOP Emi). (b) 1990 to 2019 JJA time series of relative changing ratio of surface concentrations for nitrogen oxidizes (NOx; red), ozone (O_3;

pale blue), hydroxyl radical (OH; yellow), and nitrate radical (NO_3; cyan). All relative changing ratios are calculated as the concentration in each year divided by the concentration in 1990.

2. The paper shows the trend of VOC and S/IVOC emissions. However, these organic compounds have substantially different SOA formation potentials. As a result, it is unclear which of these compounds dominate the trend of ASOA abundance. A sensitivity analysis showing the contributions of these precursors to SOA would be helpful.

Response: Thanks for the suggestion. To determine which compound dominated the trend in ASOA, we conducted two sensitivity simulations for year 1990 and 2019 by turning off anthropogenic IVOC and SVOC emissions, respectively. The simulation results showed that in 1990, SVOC accounted for 51.9% of the total ASOA, dominating its formation (Fig. S10(c)). The contribution gradually dropped to 31.8% by 2019 (Fig. S10(d)) due to emission reduction (Fig. 6(b)). Over the study period, both the absolute concentration and relative contribution of IVOC increased. Notably, the significant increase in AVOC emissions during the study period also enhanced its contribution to SOA (Fig. 6(a)). Therefore, even though SVOC emissions decreased, the rise in AVOC emissions was able to offset this decline and continued to drive the upward trend in ASOA.

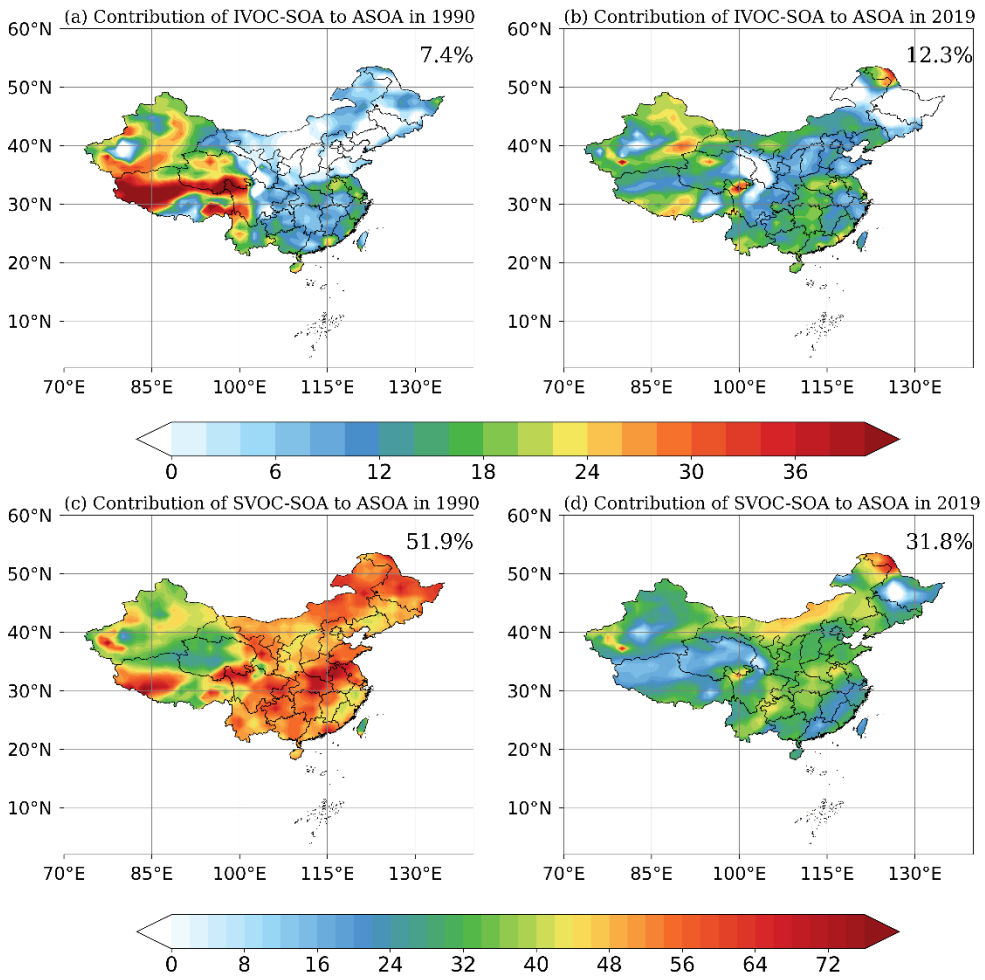

Figure S10. (a-b) Contribution of secondary organic aerosols derived from intermediate-volatile organic compounds (IVOC-SOA) to secondary organic aerosols from anthropogenic sources (ASOA) in 1990 and 2019 (unit: %). (c-d) Contribution of secondary organic aerosols derived from semi-volatile organic compounds (SVOC-SOA) to secondary organic aerosols from anthropogenic sources (ASOA) in 1990 and 2019 (unit: %). Spatial averages are shown in the upper right corner.

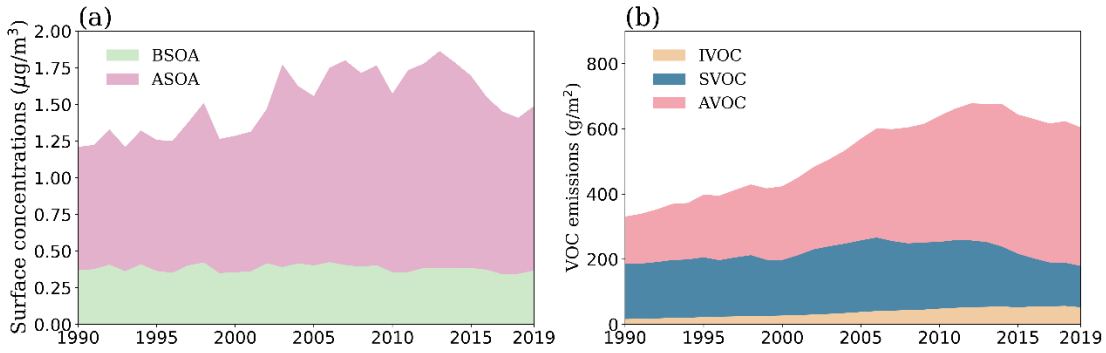

Figure 6: (a) Interannual variations in modelled average surface concentrations of secondary organic aerosols from anthropogenic sources (ASOA) and biogenic sources (BSOA) (unit: μg m^{-3}). (b) Interannual variations in emissions of aromatics (AVOC), semi-volatile organic compounds (SVOC), and intermediate-volatile organic compounds (IVOC) (unit: g m^{-2} mon^{-1}).

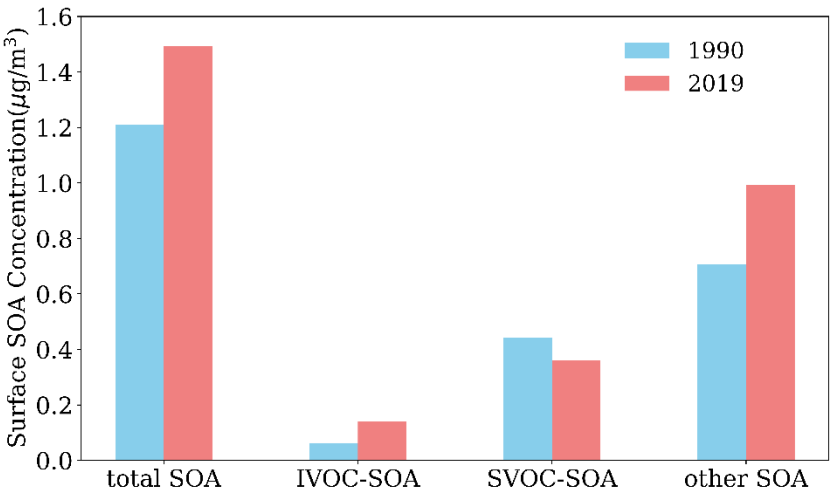

Figure S12. Annual surface secondary organic aerosols (SOA) concentrations (unit: μg m^{-3}) for total SOA, secondary organic aerosols derived from intermediate-volatile organic compounds (IVOC-SOA), secondary organic aerosols derived from semi-volatile organic compounds (SVOC-SOA), and other SOA in 1990 (blue) and 2019 (red).

3. Figure 8b shows that O3 in China did not increase significantly, which seems contrary to my understanding. Is this due to the nation-wide average vs. urban areas, where monitoring sites are located?

Response: Thanks for the comment. Figure 8b shows the normalized oxidant mixing ratios instead of the absolute concentrations. Due to the large differences in the absolute concentrations of the four oxidants, directly plotting them on the same graph may compromise the comparison. Therefore, we used the ratio calculated as the concentration in each year divided by the concentration in 1990 to demonstrate the relative changes. This allows for a clearer presentation of the trends in the different oxidants and facilitates a more effective comparison. If the analysis were based on absolute concentrations, such as examining the summer average O_3 concentrations from 2000 to 2019 (Fig.X), a significant increase can be identified. We have rephrased the caption of Fig.8b to avoid misunderstanding.

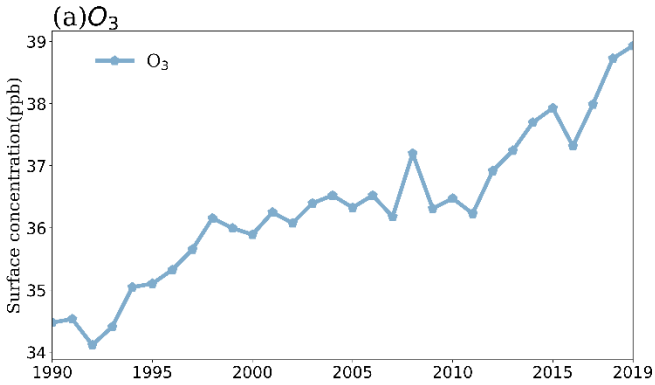

Figure X. 1990 to 2019 interannual variation of average surface ozone (O_3) (unit: ppb).

The O3 concentrations in Fig. S20 appear unreasonably high—please verify the results.

Response: Thank you for pointing this out. There was indeed a bug in plotting the O_3 concentrations. We have fixed it and replot the figure.

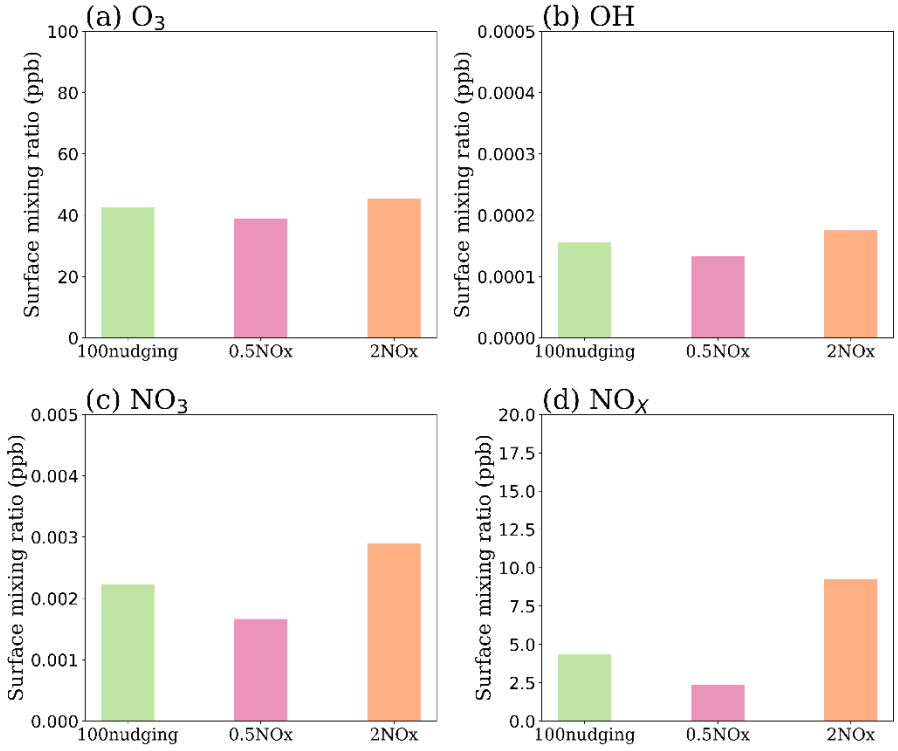

Figure S22(This figure was originally Figure S20). Surface concentrations (unit: ppb) of (a) O_3, (b) OH, (c) NO_3 and (d) NOx for July 2013 from the NOx sensitivity experiments named 100nudging (green bar), 0.5NOx (pink bar) and 2NOx (orange bar).

Additionally, Fig. 9b shows that SOA contributions from different oxidants do not change with the oxidant. For instance, all oxidants decrease in the 0.5NOx case, while SOAMT_O3 and SOAMT_NO3 increase, and SOAMT_OH decreases. Could you clarify this?

Response: Thank you for pointing this out. Fig.9(b) was mis-labelled for SOAMT_NO3 and SOAMT_OH (low NOx). We have replaced them with the correct plots (as shown below) and corrected the description in Line399-Line406. In the 0.5NOx case, atmospheric concentrations of major oxidants, including O3, OH radicals, NO3 radicals, and NOx, show corresponding reductions with decreased NOx emissions (Fig.S22), which leads to an increase in isoprene and monoterpenes concentrations (Fig.S21). As shown in Fig. 9(b) and Fig. S21, SOAMT_O3 and SOAMT_OH (low NOx) concentrations show consistent changes with monoterpenes concentrations. However, SOAMT_NO3 and SOAMT_OH (high NOx) concentrations are more strongly influenced by the decrease in NOx emissions. In addition, decreases in SOAMT_NO3 and SOAMT_OH (high NOx) concentrations were offset by increases in SOAMT_O3 and SOAMT_OH (low NOx) concentrations, which resulted in a slight increase in total surface SOAMT concentrations in response to decreasing NOx emissions (Fig.S23(c)).

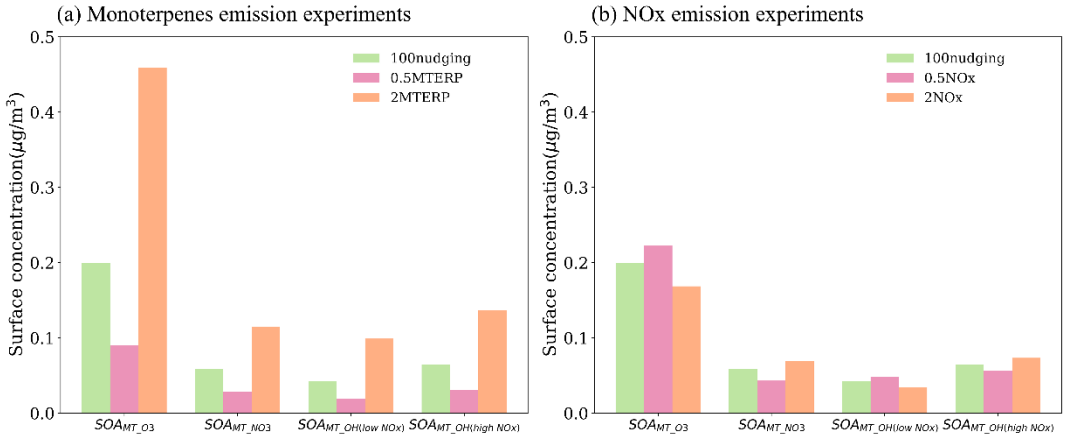

Figure 9: Surface concentrations (unit: μg m^{-3}) of monoterpene-derived secondary organic aerosols (SOA_{MT}) compositions for July 2013 from the monoterpenes (a) and NOx (b) sensitivity experiments named 100nudging (green bar), 0.5MTERP/NOx (pink bar), and 2MTERP/NOx (orange bar).

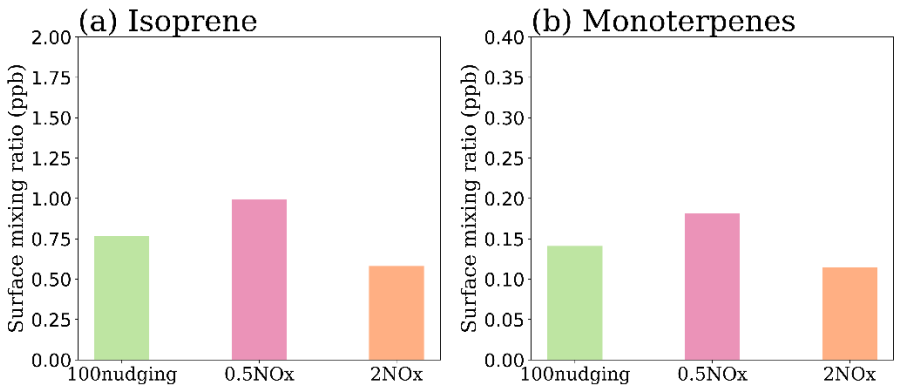

Figure S21. Surface concentrations (unit: ppb) of (a) isoprene and (b) monoterpenes for July 2013 from the NOx sensitivity experiments named 100nudging (green bar), 0.5NOx (pink bar) and 2NOx (orange bar).

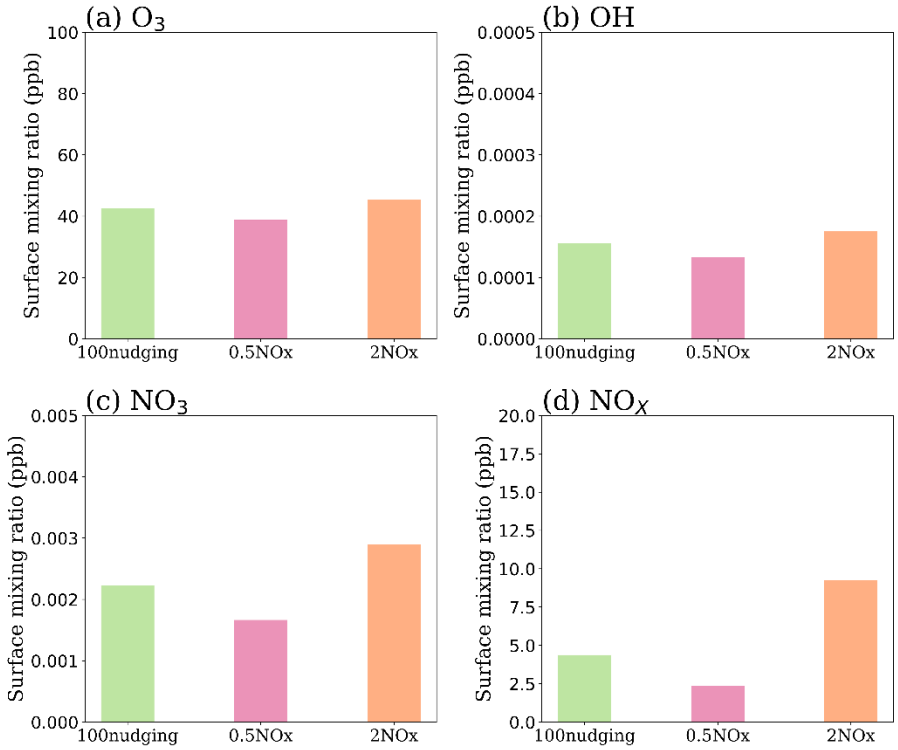

Figure S22. Surface concentrations (unit: ppb) of (a) O_3, (b) OH, (c) NO_3 and (d) NOx for July 2013 from the NOx sensitivity experiments named 100nudging (green bar), 0.5NOx (pink bar) and 2NOx (orange bar).

References

Emmerson, K. M., Cope, M. E., Galbally, I. E., Lee, S., and Nelson, P. F.: Isoprene and monoterpene emissions in south-east Australia: comparison of a multi-layer canopy model with MEGAN and with atmospheric observations, Atmos. Chem. Phys., 18, 7539–7556, https://doi.org/10.5194/acp-18-7539-2018, 2018.

Emmons, L. K., Schwantes, R. H., Orlando, J. J., Tyndall, G., Kinnison, D., Lamarque, J., Marsh, D., Mills, M. J., Tilmes, S., Bardeen, C., Buchholz, R. R., Conley, A., Gettelman, A., Garcia, R., Simpson, I., Blake, D. R., Meinardi, S., and Pétron, G.: The Chemistry Mechanism in the Community Earth System Model Version 2 (CESM2), J Adv Model Earth Syst, 12, e2019MS001882, https://doi.org/10.1029/2019MS001882, 2020.

Fu, Y. and Liao, H.: Impacts of land use and land cover changes on biogenic emissions of volatile organic compounds in China from the late 1980s to the mid-2000s: implications for tropospheric ozone and secondary organic aerosol, Tellus B: Chemical and Physical Meteorology, 66, 24987, https://doi.org/10.3402/tellusb.v66.24987, 2014.

Guenther, A. B., Jiang, X., Heald, C. L., Sakulyanontvittaya, T., Duhl, T., Emmons, L. K., and Wang, X.: The Model of Emissions of Gases and Aerosols from Nature version 2.1 (MEGAN2.1): an extended and updated framework for modeling biogenic emissions, Geosci. Model Dev., 5, 1471–1492, https://doi.org/10.5194/gmd-5-1471-2012, 2012.

Guo, J., Gong, P., Dronova, I., and Zhu, Z.: Forest cover change in China from 2000 to 2016, International Journal of Remote Sensing, 43, 593–606, https://doi.org/10.1080/01431161.2021.2022804, 2022.

Nemani, R. R., Running, S. W., Pielke, R. A., and Chase, T. N.: Global vegetation cover changes from coarse resolution satellite data, J. Geophys. Res., 101, 7157–7162, https://doi.org/10.1029/95JD02138, 1996.

Wang, H., Lu, X., Seco, R., Stavrakou, T., Karl, T., Jiang, X., Gu, L., and Guenther, A. B.: Modeling Isoprene Emission Response to Drought and Heatwaves Within MEGAN Using Evapotranspiration Data and by Coupling With the Community Land Model, J Adv Model Earth Syst, 14, e2022MS003174, https://doi.org/10.1029/2022MS003174, 2022.

Yin, H., Pflugmacher, D., Li, A., Li, Z., and Hostert, P.: Land use and land cover change in Inner Mongolia - understanding the effects of China's re-vegetation programs, Remote Sensing of Environment, 204, 918–930, https://doi.org/10.1016/j.rse.2017.08.030, 2018.